CPW Fed Monopole Antenna for Future UWB Diversity Application

Jasni A
PG Scholar, Dept of ECE
Muslim Association College of Engineering
Trivandrum, India

Mrs. Jaseem A N
Assistant Professor, Dept of ECE
Muslim Association College of Engineering
Trivandrum, India

***Abstract*— A semi-circle monopole printed antenna is proposed. The antenna consists of two identical monopoles that are printed on a low-loss substrate with 3 mm spacing and positioned perpe- ndicular to each other. Both frequency and time domain results have been measured and presented to validate the design. Result show that the proposed antenna has not only ultra-wide bandwi- dth, but also Good port isolation above 22 dB over the entire ba- nd of interest. Moreover, the radiation pattern demonstrate good orthogonal polarization operation. Furthermore, the system fi- delity factor is adequate for pulse transmission with averages of 85% and 75% for port 1 and 2, respectively. Finally, the envelope correlation coefficient has been calculated to evaluate the diversity performance. Results indicate that envelope correlation coefficient is less than 20 dB across the ultra-wide bandwidth. These results show the suitability of the proposed antenna for future UWB diversity applications.**

Keywords— ***Coplanar-fed, frequency- and time-domain, polarization diversity, ultrawideband antenna.***

I. INTRODUCTION

A new compact coplanar-fed antenna suitable for polarization diversity in ultra wideband (UWB) applications is presented. Antenna diversity is an effective solution to mitigate multipath fading signals and enhance the system capacity. Several types of diversity such as spatial/space, pattern, and polarization diversity have been proposed and implemented to simultaneo- usly receive multiple transmissions. Recently, ultra wideband (UWB) has become one of the most favorable technologies for wireless communications owing to its promising features such as low susceptibility to multipath fading, reduced probability of detection and intercept, and potentially high data rates. These make it attractive for wireless body area networks (WBANs). Various types of Printed UWB diversity antennas have been investigated and presented aiming at reducing the antenna size and increasing the isolation. The studies shows that, in body proximity scenarios, UWB-WBAN antennas excited by coplanar waveguide (CPWs) are preferred to microstrip (MS) feeding structures as they detune less near the human body. A few UWB diversity antennas among previous studies have used CPWs as the feeding structure. The antenna presented in is large in size (80* 80 mm^2) and not aimed to wearable applications, although it has an isolation better than 15 dB between its ports. A right angled triangle slot antenna employing polarization diversity was proposed. It has a compact size of 56* 56 mm^2 and above 20 dB isolation. A flexible polarization diversity antenna with small size of 34 *49 mm^2 and high isolation of 20 dB has been reported.

The two UWB tapered slot antennas (TSAs) were printed on the same substrate with a spacing of 0.5 and 0.34 free-space wavelengths at FCC center frequency (6.85 GHz) to keep the mutual coupling below -15 dB. That design employs a spatial diversity technique and, to the authors' knowledge, has the smallest size (27*47 mm^2) among the recently designed UWB diversity antennas fed by CPWs. It should be stated that although a printed cantor set fractal antenna employing spatial diversity, has a smaller size (25*48 mm^2), its bandwidth is 80% of the UWB frequency defined range.

In this letter, a new compact coplanar-fed UWB antenna aimed at applications requiring polarization diversity, like body-centric and multiple-input–multiple-output (MIMO) communications, is proposed. The whole structure has the advantage of lower mutual coupling (isolation dB) in its entire bandwidth. The proposed antenna is smaller than other previous UWB diversity CPW-fed designs. In this work, both frequency- and time-domain results have been measured and are presented in terms of S-parameters, radiation pattern, impulse response, and system fidelity factor. We also investigate the diversity performance of the proposed antenna by calculating its envelope correlation coefficient,

II. ANTENNA STRUCTURE AND DESIGN

A. Antenna Structure

Fig. 1(a) shows the geometry of the proposed antenna. It comprises two identical monopoles are perpendicular to each other and printed on a low-loss RT/DUROID 5870 substrate with a spacing of 3 mm. Each patch comprises a semicircle with a rectangular section on the top. The two branches' are fed through 50ohm coplanar lines. The back side of the substrate is devoid of metallization. The total area of the antenna structure is 27* 52 mm^2 ;the detailed dimensions are given in Table I. A photograph of the fabricated antenna is shown in Fig. 1(b).

Parameter	a	b	c	d	r	w	i	k
value–*mm*	52	27	4.5	11.4	11	3.2	0.15	0.1

TABLE I: Antenna Dimension

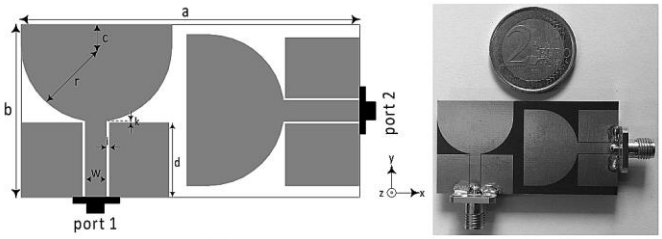

Fig.1. proposed antenna (a) geometry (b) prototype photograph

B. Antenna Operation

In order to demonstrate the antenna operation, the simulated
current distribution on the antenna at 6.85 GHz is depicted in Fig. 2. The colors representing the current distribution go
from dark blue (weak current density) to green, yellow, and red (strong current density). Fig. 2(a) and (b) shows the surface current vector when ports 2 and 1 are terminated with a 50ohm load, respectively. It is observed that when the antenna port 2 is matched, the current vector is aligned with the -axis, which leads to an -field linear -polarization; with a port 1 matched, the current vector is aligned in the -axis, which leads to a linear -polarization. It is also seen that the coupled fields to the adjacent branch are aligned with the excited port fields.

In order to show how the antenna was designed aiming at optimizing its performance, the effects of key parameters on the antenna -parameters are examined. To understand the effect of the radiating element, the semicircle radius "r" and width of the rectangular section "c" are parameterized. By changing the radius, the length of the rectangular section(2r) is also modified. Parameter "r" was kept constant and "c" changed, and then vice versa.

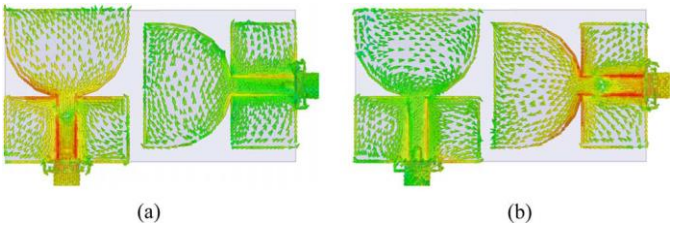

Fig.2. Current Distribution at 6.85GHz: (a) Port 2 is matched (b) port 1 is matched.

Fig. 3 shows the -parameters results as these parameters vary. As observed, decreasing "r" from 11 mm to 9 and 7 mm leads to 9.3% and 14.8% up shift in the 10-dB lower frequency edge of S_{11} and S_{22}, respectively, which reduces each antenna port matching bandwidth. Moreover, decreasing "c" (which increases the spacing between the two branches) from 4.5 mm to 2.5 and 0.5 mm results in a S_{11}lower-frequency edge upshift of 12.8% and 15%, and a S_{22}upshift of 17% and 22.7%, significantly reducing each antenna port bandwidth. It is also seen that is below 20 dB for these parameters variations. Another important parameter needing investigation is the feed-gap distance ("k") between the radiator and the CPW ground. For this purpose, the CPW ground length "d" is varied.

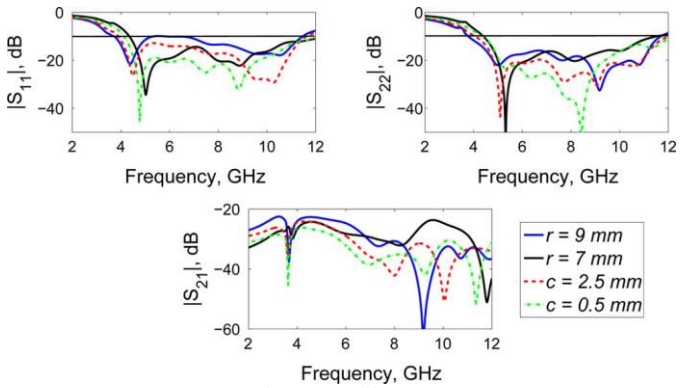

Fig.3. Simulated antenna reflection coefficients (|S11| and |S22|) and mutual coupling (|S21|) as an function of antenna parameters "r" and "c".

Simulation results depicted in Fig. 4 show that decreasing the value of "d" leads to losing the ultra-wide bandwidth behavior of port 1 and to decreasing both lower- and higher-frequency edges of port 2, while the isolation is at any case above -20 dB.

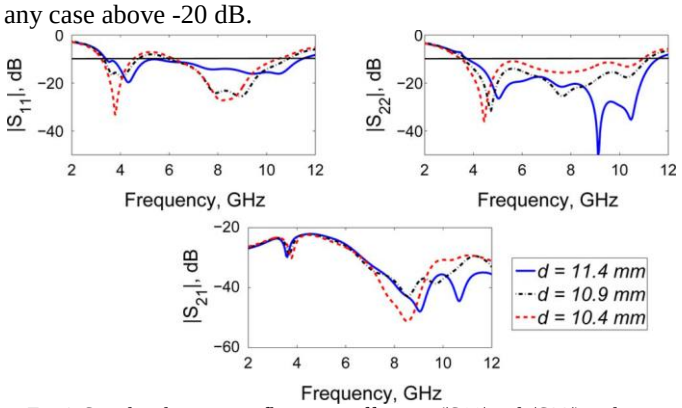

Fig.4. Simulated antenna reflection coefficients (|S11| and |S22|) and mutual coupling (|S21|) as an function of antenna parameters "d".

III. EXPERIMENTAL RESULTS

In order to validate the proposed design, both frequency- and
time-domain measured results including -parameters, radiation
pattern, impulse response, and system fidelity factor, are presented.:

A. Ultra-wide matching bandwidth and Isolation

Measured and simulated antenna -parameters are depicted in Fig. 5. As it can be seen, reflection coefficient impedance bandwidths, based on |S11|and |S22| 10 dB (almost in the entire band except at 7–7.4 GHz where reaches a maximum of 9.5 dB at 7.2 GHz), of port 1 and port 2 are 3.25–12 GHz (115%) and 3.55–11.7 GHz (107%) , respectively. Moreover, is lower than 22 dB over the entire range of frequencies. The discrepancy between simulated and measured -parameters responses is attributed to factors such as imperfect solder joints of the SMA connector to the feedline and manufacturing tolerances. Additionally, the induced currents on the feeding cable, due to the ground issues of small antennas , cause the extra resonances in Fig. 5(b). However, when the antenna is connected to the transceiver systems, there will be no feeding cable. The experimental results confirm the ultra-

wide matching bandwidth of the proposed diversity antenna with a good isolation between its ports.

B. Radiation Patterns

Fig. 6 depicts the measured radiation patterns at 3.1, 6.85, and
10.6 GHz when port 2 is excited, while port 1 is terminated with a 50- load, and vice versa.

It is observed that the patterns for the excitation at port 2 are approximately a 90 rotation of the case when port 1 is excited, showing a good orthogonal polarization operation. Note that since the direct feed radiation pattern is somewhat blocked (between 0, –180) by the other branch and SMA ended with 50ohm load, the known effects of increasing side lobes and nulls is seen in both planes, especially at higher frequencies.

Note that the blockage effects are moderate when port 2 is excited, owing to the port 1 location that is not directly in line of sight of the transmitter.

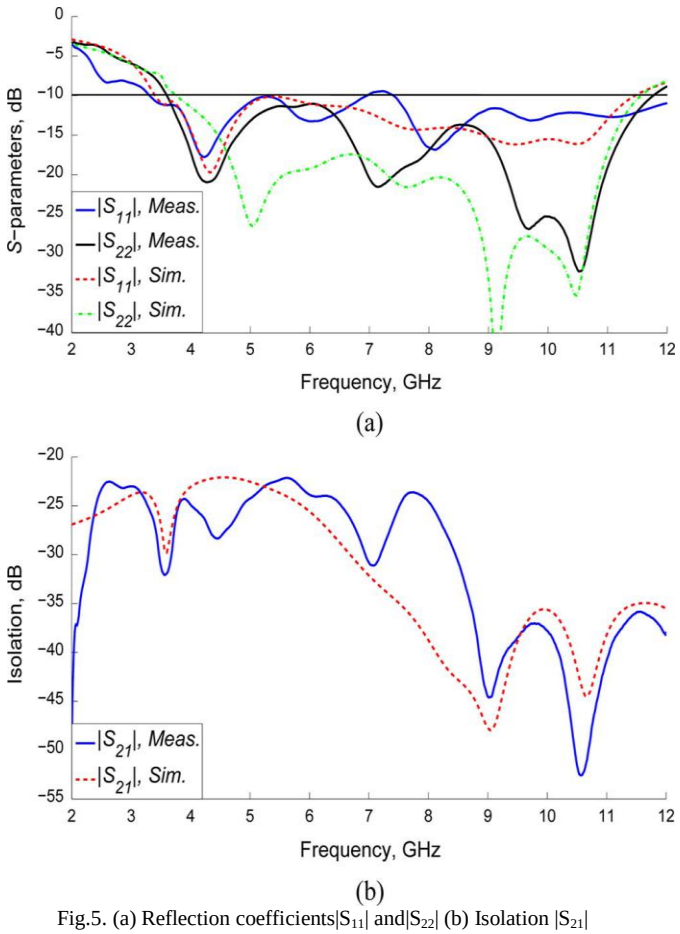

Fig.5. (a) Reflection coefficients$|S_{11}|$ and$|S_{22}|$ (b) Isolation $|S_{21}|$

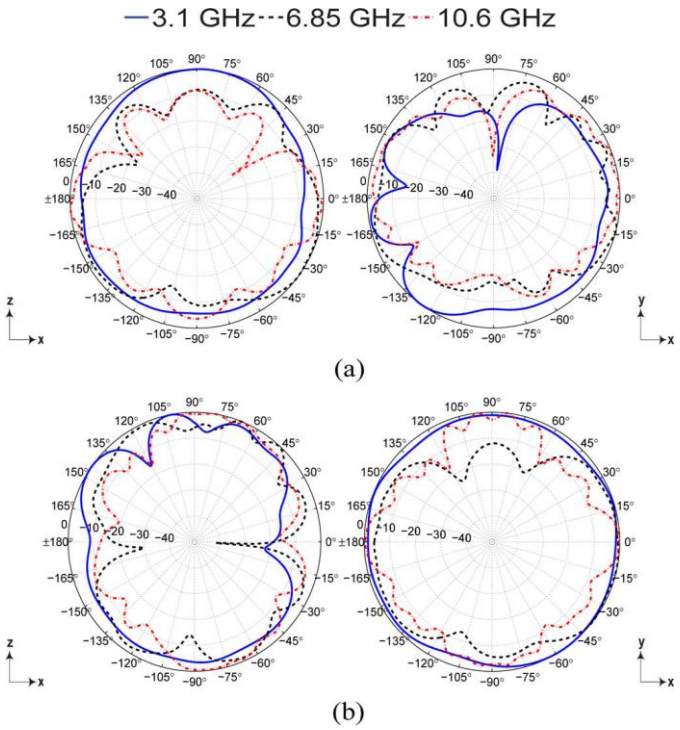

Fig.6. Measured patterns at 3.1,6.85, 10.6 GHz (a) port 2 is matched (b) port 1 is matched

C. Block Diagram

The time-domain setup selected in this letter comprises two identical diversity antennas, one for transmitting (Tx) and one
for receiving (Rx), placed with a large enough separation distance(30 cm) to be considered in the far field of each other.
During measurement, the antennas' ports 1 are connected to the vector network analyzer (VNA), while ports 2 are terminated with 50ohm loads, and vice versa. To investigate the system behavior in different directions, the two antennas' time performance was measured in different orientations (and 90degree); the Tx antenna is fixed, while the Rx antenna rotates in the azimuth plane. The 90 rotation is made for each port of the Rx antenna aligned with the related port axis (for port 1 and for port 2), as seen in Fig. 7.

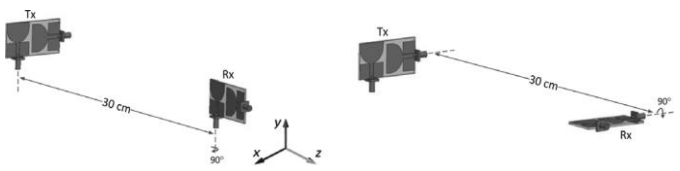

Fig.7. For 90° rotation (a) ports 2 are matched (b) ports 1 are matched.

To have the transient behavior, time-domain data were extracted from frequency-domain -parameters measurements
using an inverse fast Fourier transform. This technique has the advantage of describing the radiation of arbitrary input signals. The CST default Gaussian modulated pulse with

spectrum covering the UWB FCC band was used as the input
signal, as it completely complies with the FCC indoor and outdoor power masks.
To quantify the level of distortion, the system fidelity factor has been calculated, and results are given in Table II. The agreement between the simulated and measured values is fairly good. The average system fidelity factors, for the considered directions, of ports 1 and 2 are 85 % and75 %, respectively, which indicate that the level of signal distortion is quite acceptable for UWB signals transmission.

Matched port	φ	System Fidelity Factor	
		Simulated	Measurec
Port 1	0°	0.732	0.865
	90°	0.769	0.832
Port 2	0°	0.745	0.782
	90°	0.682	0.708

TABLE II : System Fidelity Factor

To evaluate the diversity performance, the envelope correlation coefficient has been computed using the equation (1).

$$\rho_e = \frac{|S_{11}^* S_{12} + S_{21}^* S_{22}|^2}{(1-(|S_{11}|^2+|S_{21}|^2))(1-(|S_{22}|^2+|S_{12}|^2))} \quad (1)$$

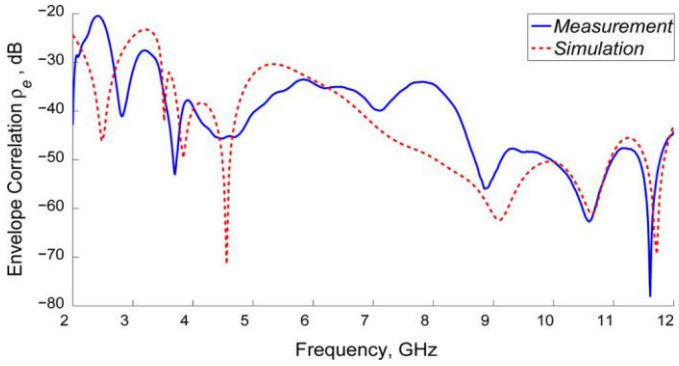

Fig.8. Measured and simulated envelope correlation

The correlations obtained for both simulated and measured results are depicted in Fig. 8. As observed, the envelope correlation coefficient for our proposed UWB diversity antenna is below 20 dB across the entire ultra-wide bandwidth. Note that the correlation at low frequencies, which is usually much higher, is still very low in our proposed diversity antenna. These results indicate the effectiveness of the designed dual orthogonal polarization, which leads to a good diversity performance.

IV. ACKNOWLEDGEMENT

I would like to express my sincere gratitude to my professors, dept of electronics and communication engineering for there valuable guidance and there encouragement in pursuing this paper.

V. CONCLUSION

A novel compact CPW-fed UWB antenna employing polarization diversity has been proposed. The antenna consists of two identical monopole base designs that are perpendicular to each other and printed on a low-loss substrate with spacing of 3 mm. The obtained bandwidth for the proposed antenna is
115% for port 1 and 107 % for port 2. Within the ultra-wide frequency range, the isolation is above 22 dB. The radiation patterns demonstrate a good orthogonal polarization operation. The calculated system fidelity factor is about 85% and 75% for port 1 and port 2, respectively. The envelope correlation coefficient, for our proposed UWB diversity antenna is below 20 dB across the entire ultra-wide bandwidth, even at the lower frequencies. These results show the suitability of the proposed antenna for future portable UWB diversity applications.

REFERENCES

1. C. B. Dietrich, Jr., K. Dietze, J. R. Nealy, and W. L. Stutzman, "Spatial, polarization, and pattern diversity for wireless handheld terminals," *IEEE Trans. Antennas Propag.*, vol. 49, no. 9, pp. 1271–1281, Sep. 2001.
2. B. Allen,M. Dohler, E. Okon,W. Q.Malik, A. K. Brown, and D. Edwards, *UWB Antenna and Propagation for Communications, Radar and Imaging*. Hoboken, NJ, USA: Wiley, 2007.
3. A.Wang, F. Zhenghe, and K.-M. Luk, "Pattern and polarization diversity antenna with high isolation for portable wireless devices," *IEEE Antennas Wireless Propag. Lett.*, vol. 8, pp. 209–211, 2009.
4. P. S. Hall and Y. Hao, *Antennas and Propagation for Body CentricCommunications Systems*. Norwood, MA, USA: Artech House, 2006.
5. E. M. Staderini, "UWB radars in medicine," *IEEE Aerosp. Electron. Syst. Mag.*, vol. 17, no. 1, pp. 13–18, Jan. 2002.
6. W. K. Toh, Z.N. Chen,Q.Xianming, and T. S. P. See, "AplanarUWB diversity antenna," *IEEE Trans. Antennas Propag.*, vol. 57, no. 11, pp. 3467–3473, Nov. 2009.
7. Sh.Zhang, Zh. Ying, J. Xiong, and S. He, "Ultra wideband MIMO/diversity antennas with a tree-like structure to enhance wideband isolation," *IEEE Antennas Wireless Propag. Lett.*, vol. 8, pp. 1279–1282, 2009.
8. T. S. P. See and Z. N. Chen, "An ultrawideband diversity antenna," *IEEE Trans. Antennas Propag.*, vol. 57, no. 6, pp. 1597–1605, Jun. 2009.
9. S. Hong, K. Chung, J. Lee, S. Jung, S.-S. Lee, and J. Choi, "Design of a diversity antenna with stubs for UWB applications," *Microw. Opt. Technol. Lett.*, vol. 50, pp. 1352–1356, 2008.
10. M. Gallo, E. Antonino-Daviu, M. Ferrando-Bataller, M. Bozzetti, J. M. Molina-Garcia-Pardo, and L. Juan-Llacer, "A broadband pattern diversity annular slot antenna," *IEEE Trans. Antennas Propag.*, vol. 60, no. 3, pp. 1596–1600, Mar. 2012.
11. L. Xiong and P. Gao, "Compact dual-polarized slot UWB antenna with CPW-fed structure," in *Proc. IEEE APS/URSI*, 2012, pp. 1–2.
12. H. K. Yoon, Y. J. Yoon, H. Kim, and C.-H. Lee, "Flexible ultra-wideband polarization diversity antenna with band-

notch function," *Microw., Antennas Propag.*, vol. 5, no. 12, pp. 1463–1470, 2011.
13. G. Augustin, B. P. Chacko, and T. A. Denidni, "Dual port ultra wideband antennas for cognitive radio and diversity applications," in *Advancement in Microstrip Antennas With Recent Applications*. Rijeka, Croatia: InTech, 2013, ch. 9.
14. Q. H. Abbasi, M. M. Khan, S. Liaqat, M. Kamran, A. Alomainy, and Y. Hao, "Experimental investigation of ultra wideband diversity Techniques for on-body radio communications," *Prog. Electromagn. Res. C*, vol. 34, pp. 165–181, 2013.
15. Q. H. Abbasi, A. Alomainy, and Y. Hao, "Ultra wideband antenna diversity techniques for on/off-body radio channel characterization," in *Proc. IEEE iWAT*, 2012, pp. 209–212.
16. Y. Li, W. X. Li, Ch. Liu, and T. Jiang, "A printed diversity cantor set fractal antenna for ultra wideband communication applications," in *Proc. Antennas, Propag., EM Theory*, 2012, pp. 34–38.
17. M. Koohestani, A. A. Moreira, and A. K. Skrivervik, "Feeding structure influence on performance of two UWB antennas near a human arm," in *Proc. 8th EuCAP*, 2014, to be published.
18. Ch. Zhi, T. S. P. See, and Q. Xianming, "Small printed ultrawideband antenna with reduced ground plane effect," *IEEE Trans. Antennas Propag.*, vol. 55, no. 2, pp. 383–388, Feb. 2007.
19. J. Liu, K. Esselle, S. Hay, Z. Sun, and S. Zhong, "A compact Superwideband antenna pair with polarization diversity," *IEEE Antennas Wireless Propag. Lett.*, vol. 12, pp. 1472–1475, 2013.
20. G. Quintero, J.-F. Zürcher, and A. K. Skrivervik, "System fidelity factor: A new method for comparing UWB antennas," *IEEE Trans. Antennas Propag.*, vol. 59, no. 7, pp. 2502–2512, Jul. 2011. factor: A new method for comparing UWB antennas," *IEEE Trans. Antennas Propag.*, vol. 59, no. 7, pp. 2502–2512, Jul. 2011.
21. M. Koohestani, N. Pires, A. K. Skrivervik, and A. A. Moreira, "Time domain performance of patch-loaded band-rejectUWB antenna," *Electron.Lett.*, vol. 49, no. 6, pp. 385–386, 2013.